A New Energy Management Strategy for Multimode Power-Split Hybrid Electric Vehicles

A New Energy Management Strategy for Multimode Power-Split Hybrid Electric Vehicles

Giuseppe Buccoliero, Pier Giuseppe Anselma, *Student Member*, *IEEE*, Saeed Amirfarhangi Bonab, Giovanni Belingardi, Ali Emadi, *Fellow*, *IEEE*

***Abstract*—Among the hybrid electric vehicle categories, the multimode power-split allows to fully exploit the advantages related to the powertrain electrification. However, together with the increased flexibility, it comes with greater difficulty in defining an effective control strategy, both in terms of predicted fuel consumption and computational cost. To overcome the limits of the most diffused energy management strategies, slope-weighted energy-based rapid control analysis (SERCA) has been recently proposed. Nevertheless, so far, the algorithm has been applied to powertrains characterized by two operative modes solely. In this paper, we first present the inconsistency of SERCA applied to the whole set of multimode power-split arrangements. Subsequently, after correlating this divergence to the mode selection process, to overcome this draft, we introduce a novel strategy called SERCA$^+$. This algorithm is proven to be robust and to achieve results close to the optimum benchmark with an insignificant increase in computational cost. Therefore, SERCA$^+$ could potentially find application in design methodologies for multimode power-split HEVs to accelerate the overall vehicle design process.**

***Index Terms*—Electric vehicles, energy management, fast analysis, hybrid, multimode, optimal control, power-split powertrain**

I. Introduction

THE new challenges of reducing fuel consumption and the pollutant emissions are leading the transport sector towards a paradigm shift. Among the sustainable alternatives to carbon fossil dependency, electrification is one of the most appealing solutions. The technological progress, especially in the power electronics field, is making electrified vehicles increasingly attractive for the mobility scenarios. Nevertheless, some know-how limitations, as the ones related to the battery energy density, represent the current obstacles for a widespread application of the fully electric vehicles (EVs). Consequently, shortly, as a temporary transition, the market will likely be dominated by hybrid electric vehicles (HEVs) [1-4].

Among the possible state of the art design architectures of the HEVs, the power-split is the most attractive category, both for heavy-duty and light-duty applications [5-8].

Indeed, it allows exploiting the advantages of both parallel and series configurations. These types of power units typically use the planetary gear sets (PGs) as the power-split devices to separate the engine power in an electrical and a mechanical path.

Moreover, the addition of clutches greatly enhances the operational flexibility, enabling multimode operations [9,10].

To maximize the advantages of the multimode powertrains, a decisive part is the control strategy which is responsible for both selecting the operative mode and determining the power flow between powertrain components [11-13]. Particularly, since many design choices are possible, to select the proper arrangement for the specific application, it is crucial to find an algorithm ensuring reliable results with low computational cost [14]. Among the strategies introduced in the literature to address the control of HEVs, the most diffused ones are dynamic programming (DP) [15], equivalent consumption minimization strategy (ECMS) [16], and Pontryagin's minimum principle (PMP) [17]. However, all these present some drawbacks when it comes to the multimode application. DP ensures global optimality by paying an excessive computational burden [15]. Both ECMS and PMP need the tuning of some parameters, which are mode dependent [18]. Zhang et al. have introduced a fast algorithm named power-weighted efficiency analysis for rapid sizing (PEARS) of HEVs [19,20]. However, as we will show in the case study section, this strategy might produce results far from the DP optimal benchmark. Therefore, an offline control strategy for a multimode power-split HEV that achieves near-optimal results in terms of fuel consumption while exhibiting reduced computational cost still needs an exhaustive development.

To address this issue, Anselma et al. have recently proposed a new methodology, called slope-weighted energy-based rapid control analysis (SERCA) [21]. This strategy has been proven to achieve good results for a dual mode transmission but has not been applied yet to the powertrains with more than two operative modes. In this paper, first we attempt to extend the SERCA methodology to the case of multimode powertrains. Nevertheless, we demonstrate the lack of consistency of this strategy in dealing with the mode choice. Consequently, we introduce another approach, called SERCA$^+$, which combines the strength of PEARS and SERCA. Finally, we present a case

G. Buccoliero is with the Department of Mechanical and Aerospace Engineering (DIMEAS), Politecnico di Torino, Torino 10129, Italy and with the McMaster Institute for Automotive Research and Technology (MacAUTO), McMaster University, Hamilton ON L8P0A6, Canada (e-mail: giuseppe.buccoliero@studenti.polito.it)

P.G. Anselma and G. Belingardi are with the Department of Mechanical and Aerospace Engineering (DIMEAS) and with the Center for Automotive Research and Sustainable Mobility (CARS), Politecnico di Torino, Torino 10129, Italy (e-mail: pier.anselma@polito.it; giovanni.belingardi@polito.it).

S.A. Bonab and A. Emadi are with the McMaster Institute for Automotive Research and Technology (MacAUTO), McMaster University, Hamilton ON L8P0A6, Canada (email: amirfars@mcmaster.ca; emadi@mcmaster.ca).

TABLE I
POWERTRAIN COMPONENTS MAIN PARAMETERS

Components	Parameters	Value
ICE	$Capacity$	3.6 L
	P_{max}	188 kW @5800 rpm
	T_{max}	320 Nm @4400 rpm
	LHV	43700 J/g
	ρ_{fuel}	737 g/l
MG1	P_{max}	60 kW
	T_{max}	123 Nm
	n_{max}	14500 rpm
MG2	P_{max}	85kW
	T_{max}	317 Nm
	n_{max}	14500 rpm
Battery	$P_{discharg_{max}}$	59 kW
	$P_{charg_{max}}$	107 kW
	V_{max}	402 V
	I_{max}	300 A
	$Energy_{max}$	64.26 MJ
Vehicle	I_v	309.6 Kgm^2
	r_{dyn}	0.3582 m
	K	2.64

study on a state-of-the-art architecture to demonstrate the benefit of the proposed solution. SERCA+ is particularly proven to achieve near-optimal results in terms of fuel consumption compared with the global optimal DP benchmark. On the other hand, compared with PEARS as the most rapid HEV control strategy, SERCA+ exhibits a minor increase in computational burden. This suggests the potential use of SERCA+ to accelerate the design process of multimode power-split HEVs.

II. Vehicle and Powertrain Model

In this section, we present the quasi-static vehicle model, implemented in our analysis. Required vehicle and powertrain parameters used for the simulation are reported in Table I.

A. Road Load Model

The road resistance force F_{road} is modelled using following equation

$$F_{load} = F_{aero} + F_{rr} \tag{1}$$

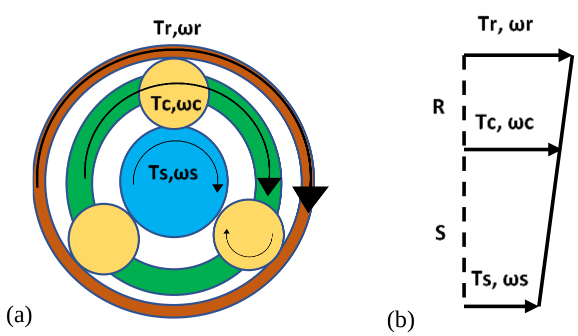

Fig. 1: Planetary gear set (a) and lever diagram (b)

where F_{areo} is the aerodynamic drag and F_{rr} is the rolling resistance.

Consequently, the road load torque on the powertrain and powertrain rotational speed are computed as

$$T_{pt} = \frac{F_{road} r_{dyn} + \frac{I_v\, a}{r_{dyn}}}{K} \tag{2}$$

$$\omega_{pt} = \frac{K \cdot v}{r_{dyn}} \tag{3}$$

where r_{dyn} is the wheel dynamic rolling radius, K is the final drive ratio, I_v is the vehicle's combined momentum of inertia at wheel, a is the longitudinal acceleration, and v is the longitudinal speed [21].

B. Planetary Gear (PG) Model

The PG device is the core element of power-split powertrains. PG is a two degrees of freedom (DOF) dynamic system. Rotational speeds of its nodes (ring, carrier and sun) are subjected to the kinematic constraint illustrated in (4). Fig.1 shows the PG device scheme and the lever analogy, which is useful dealing with architectures with multiple PGs [22].

$$\omega_s r_s + \omega_r r_r = \omega_c (r_r + r_s) \tag{4}$$

We assume that forces exchanged between PG nodes are the same due to the small gear inertia assumption [23] and that the inertia of powertrain components are negligible compared to the vehicle one [19]. Under these hypotheses, equations for the PG torque are derived as [24]

$$\frac{T_s}{T_c} = -\frac{R_s}{R_r + R_s} \qquad \frac{T_r}{T_c} = -\frac{R_r}{R_r + R_s} \tag{5}$$

Where subscripts $s, c,$ and r are used to identify sun, carrier, and ring, respectively, and T and ω represent the torque and speed for the nodes. In this paper, we focus on powertrains with double PG arrangement. In fact, previous researches have proven the benefits of this choice for light-duty applications [25].

C. Model of the Powertrain Components

The internal combustion engine (ICE) and the motor generator units (MGUs) are modeled using experimentally derived steady-state look-up tables. For the ICE, the map refers to the amount of fuel consumption as a function of torque and speed. Instead, for the MGUs, the map shows the power losses as a function of torque and speed. Finally, the battery is modeled by an equivalent circuit model, where the value of the internal resistance (R_{int}) and the open circuit voltage (V_{OC}) are assumed constant respective to variation in the battery state of charge (SOC), state of health (SOH), and temperature. In fact, it has been demonstrated how these hypotheses allow to reach results with a good level of approximation [17, 26]. The battery power is computed using (6)

$$P_{batt} = \sum_{i=1}^{2} \omega_{MGi}\, T_{MGi}\, \eta_{MGi}^{-sign\,(\omega_{MGi} T_{MGi})} \tag{6}$$

where η denotes the efficiency of the motor generator units.

III. MULTIMODE POWER-SPLIT HEV CONTROL

In this section, we discuss the control strategies which have been presented in the literature to deal with the energy management problem for the studied hybrid electric powertrain category.

A. Dynamic Programming (DP)

Optimal control problem for the energy management of a multimode power-split HEV powertrain can be written as (7) in which time is discretized in N steps with a time step of Δt. The objective function is also considered as the integration of a discrete cost function, $J\,(T_{ICE}[k], \omega_{ICE}[k])$, which is the amount of fuel consumption rate at each time step.

$$J^* = min \sum_{k=0}^{N-1} J(T_{ICE}[k], \omega_{ICE}[k])\,\Delta t$$

subject to

$$\begin{gathered} SOC[0] = SOC[N] \\ SOC_{min} \leq SOC[k] \leq SOC_{max} \\ SOC[k+1] = SOC[k] - \frac{P_b[k]\Delta t}{V_b Q_b} \\ P_{load}[k] \leq P_{ICE}[k] + P_{MG1}[k] + P_{MG2}[k] \\ \\ P_b[k] = P_{MG1,e}[k] + P_{MG2,e}[k] \\ P_{MG1,e} = f_1(T_{MG1}[k], \omega_{MG1}[k]) + P_{MG1} \\ P_{MG2,e} = f_2(T_{MG2}[k], \omega_{MG2}[k]) + P_{MG2} \\ P_{b,min} \leq P_b[k] \leq P_{b,max} \\ \omega_{ICE,max} \leq \omega_{ICE}[k] \leq \omega_{ICE,min} \\ \omega_{MG1,max} \leq \omega_{MG1}[k] \leq \omega_{MG1,min} \\ \omega_{MG2,max} \leq \omega_{MG2}[k] \leq \omega_{MG2,min} \\ T_{ICE,max} \leq T_{ICE}[k] \leq T_{ICE,min} \\ T_{MG1,max} \leq T_{MG1}[k] \leq T_{MG1,min} \\ T_{MG2,max} \leq T_{MG2}[k] \leq T_{MG2,min} \end{gathered} \tag{7}$$

where P_b, V_b, and Q_b are battery power, voltage, and capacity, respectively. Also $P_{MG1,e}$ and $P_{MG2,e}$ denote electrical power for the first and second motor generator and functions f_1, f_2, and J are lookup tables for the MG1, MG2, and the ICE, respectively. Moreover, while forming the optimal control problem, we have assumed that reference vehicle speed is given as a driving cycle to follow. Based on this assumption, we calculate the P_{load} for each time step as

$$P_{load}[k] = T_{pt}[k] \cdot \omega_{pt}[k] \tag{8}$$

We should also note that we have a set of quasi-static equations for the power-split device in the following format

$$PS \cdot \begin{bmatrix} \mathbf{T} \\ \boldsymbol{\omega} \end{bmatrix} = \mathbf{0} \tag{9}$$

In this equation, PS is the power-split device matrix, which changes accordingly with different architectures and the operating modes. Also, $\mathbf{T}$ is the vector of components torque, including T_{ICE}, T_{MG1}, and T_{MG2}. Also, $\boldsymbol{\omega}$ is the vector of the rotational speeds of the components. During DP implementation for the vehicle, state variable is always the SOC, however, control inputs will be chosen from the torque and speed for ICE, MG1, MG2, depending on the degree of freedoms for the power-split device. This in turn, depends on the architecture, topology, and the operating mode.

DP is a numerical method which guarantees the achievement of the optimal solution by exhaustively considering all the possible solutions. To implement DP, time, control inputs, and the state variables need to be discretized. Consequently, obtained optimal results depend on the grid resolution. In this paper, due to the high computational cost, we consider DP results as a benchmark for the other EMS [18].

B. Power-Efficiency Analysis for Rapid Sizing (PEARS)

The PEARS algorithm has been introduced ad hoc to deal with the design of multimode power-split HEV powertrains, adopting a charge sustaining (CS) strategy to manage the battery energy. This heuristic approach relies on the idea that each component should work as close as possible to its best efficiency region to achieve good sub-optimal performance. For each driving cycle point, the best EV (ICE off or pure electric) and HEV (ICE on) working conditions are selected on the base of the efficiency definitions reported in (10) and (11).

$$\begin{gathered} \eta_{EV} = 1 - \frac{P_{EV}^{loss}}{P_{EV}^{in}} \\ \eta_{EV}^*|_{\omega_{out},\dot{\omega}_{out}} = max[\eta_{EV}\ (T_{MG1}, T_{MG2})]|_{\omega_{out},T_{demand}} \end{gathered} \tag{10}$$

$$\begin{aligned} \eta_{HEV}(\omega_e, T_e) &= \frac{P_{ICE1}\,\eta_G\eta_{batt} / \eta_{ICEmax}\,\eta_{Gmax}}{P_{fuel} + \mu P_{batt}} \\ &+ \frac{P_{ICE2}\,\eta_G\eta_M / \eta_{ICEmax}\,\eta_{Gmax}\,\eta_{Mmax}}{P_{fuel} + \mu P_{batt}} \\ &+ \frac{P_{ICE2} / \eta_{ICEmax} + \mu P_{batt}\eta_{batt}\eta_M / \eta_{Mmax}}{P_{fuel} + \mu P_{batt}} \\ \eta_{HEV}^*|_{\omega_{out},\dot{\omega}_{out}} &= max[\eta_{HEV}\ (\omega_{ICE}, T_{ICE})]|_{\omega_{out},T_{demand}} \end{aligned} \tag{11}$$

In these formulations, P_{EV}^{loss} and P_{EV}^{in} denote the electrical losses and the electrical power flowing into the system, respectively, η denotes the efficiency, and μ is a banner for battery energy employment. Additionally, as illustrated in Fig. 2, P_{ICE1}, P_{ICE2}, and P_{ICE3} are the fractions of engine power to reach the battery, electric motor, and final drive respectively.

At each driving cycle point, the best EV mode is selected first. Then, the HEV modes are iteratively substituted based on the efficiency difference with the pure electric counterparts

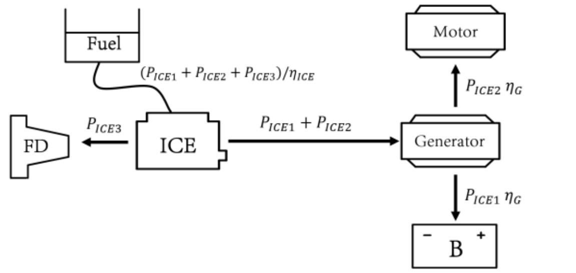

Fig. 2: Schematic of power flow from engine to the generator, battery, motor, and the final drive with fractions shown as P_{ICE1}, P_{ICE2}, and P_{ICE3}. Note that η_{ICE} and η_G are the engine and generator efficiency, respectively.

[19]. Different versions of the algorithm have been proposed in the literature. The first, called PEARS$^+$, uses the DP for the mode selection and the PEARS for the torque split determination, thus partially compromising the computational cost advantage [27,28]. In the second version, a penalty function has been introduced to mitigate the effects of the mode schedule [29,30]. In this paper, we refer to this latter version of the PEARS strategy. Despite its computational advantage, the major drawback of the PEARS algorithm refers to its non-uniform proximity with optimal results from DP, as demonstrated in [21] and later in this paper.

IV. Slope-weighted Energy-based Rapid Control Analysis (SERCA) for Dual Mode Application

To overcome the PEARS limitations, Anselma et al. introduced a new approach, SERCA [21]. The procedures related to this strategy can be summarized in three main steps.

1) STEP 1: Subproblem Exploration

During the first step, all the possible solutions are explored. At each driving cycle point, the best EV mode is chosen according to the same efficiency definition reported in the PEARS, (10). For the HEV modes, fuel consumption and battery usage are identified for any feasible working point for the powertrain. Working points differ in terms of torque and speed of the powertrain components. This step results in a point cluster, similar to Fig. 3.

The lower edge of this point cluster contains the possible optimal solutions. In fact, fixing the amount of fuel consumption, points on this edge have the lowest $-\Delta SOC$, which means charging the battery as much as possible. Consequently, this edge forms a pareto-optimal front [31].

2) STEP 2: Generalized optimal point definition

In the second step, for the HEV mode (the mode with ICE on), the fuel consumption axis is discretized, as shown in Fig. 3. The resolution is decided as a trade-off between computation burden and the accuracy. For each interval, the point in the pareto-optimal front with lowest $-\Delta SOC$ is selected to represent all other points in that interval. Also, working condition, which is the torque and speed of components, is captured for the selected point. Repeating this procedure would result in a single point for each interval of fuel consumption (FC). These points are shown as red circles in Fig. 4 (a). Connecting these points

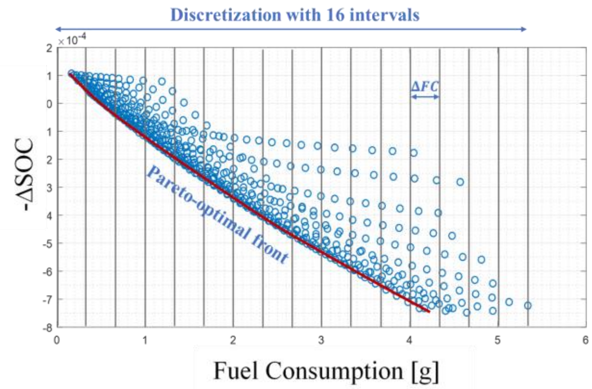

Fig. 3: Examples of all feasible working points, discretization intervals, and pareto-optimal front, for a driving cycle points.

would result in a piece-wise linear envelope, which the point in the far left represents the EV mode (Fig. 4 (a)). In the piece-wise linear envelope, we are interested in linear segments with high $|\Delta SOC/FC|$ ratios, since these segments have less FC for the same change in SOC. Therefore, we filter the piece-wise linear envelope to get a convex envelope (Fig. 4 (b)). In the convex envelope, each connecting segment (blue lines in Fig. 4 (b)) have a slope, decreasing in absolute value moving from left to right. We label the current driving cycle point with the first slope of the convex envelope (the one in far left).

3) STEP 3: Energy balance realization

In the last step, as for the PEARS, first, the best EV points are chosen for all driving cycle points. Obviously, this solution is not a CS solution. To address this, the substitution process is then performed for the driving cycle point with the highest labeled slope value, in which EV mode is replaced with a HEV mode. The labeled slope for that driving cycle point is also updated and replaced with the second slope value. This process continues iteratively and terminates as soon as the CS solution is achieved. Final CS solution is a set of HEV/EV points, for which the working condition is completely known.

V. Limitations of SERCA for Multimode HEVs

In this section, we present drawbacks that occur when attempting to straightforwardly apply the SERCA methodology for powertrains with more than two operative modes. We present the algorithm procedures in the same order as for the dual mode case.

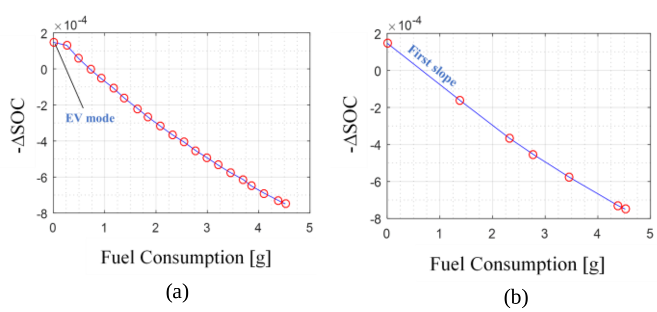

Fig. 4: (a) selected points for the intervals, connected to form the piece-wise linear front. (b) convex envelope as a result of filtering out the concavities in the piece-wise linear envelope.

1) STEP 1: Subproblem Exploration

For a dual mode powertrain, at each driving cycle point, the EV mode capable of achieving the highest efficiency is selected. Then, a single cluster of operating points is formed for each HEV mode.

2) STEP 2: Generalized optimal point definition

During the second phase, the clusters are transformed into envelopes of piece-wise linear functions. At each driving cycle point, the starting vertex for the profiles is the best EV mode, identified from the previous step. Finally, the envelope is filtered to ensure the convexity. As shown in Fig. 5, the result is a set of different convex envelopes (one for each HEV mode) sharing the starting point.

3) STEP 3: Energy balance realization

In the last step, the mode shifting strategy and power split policy are chosen. Once more, first, the best EV mode is picked for each driving cycle point. When no feasible EV is present, the algorithm chooses the HEV mode with the lowest fuel consumption. Subsequently, the total electrical energy required to achieve CS condition is computed. The iterative substitution of the HEV modes follows the order identified by the steepest slope. However, unlike the dual case explained before, a crucial step is to update the common starting point (see Fig. 5) to the newly selected HEV point. Also, before moving to the next iteration, since the initial point has been changed for the HEV working conditions, the filtering criteria need to be re-applied.

Despite the good performances of SERCA for dual-mode powertrains [21], the implementation for the multimode case has shown some limits of the method. We have found a strong dependency of multimode SERCA on two tuning factors: the number of intervals selected for torque and speed sweep of the components and the size of the discretization in fuel consumption. The algorithm generates inconsistent results when increasing the number of mesh intervals, which undermines the accuracy of the results. In Fig.6, examples of fuel consumption variation with respect to the tuning parameters in the UDDS driving cycle are reported for two multimode arrangements. The results seem to be case-independent, since the same trend has been observed analyzing other multimode arrangements as well.

Additionally, SERCA results for multimode arrangement shows excessive changes in the modes of operation. Proposed

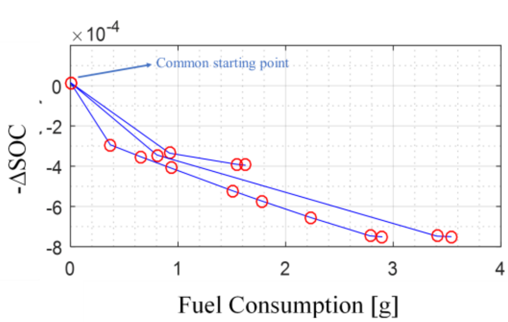

Fig. 5: Example of SERCA envelopes for a three HEV mode powertrain.

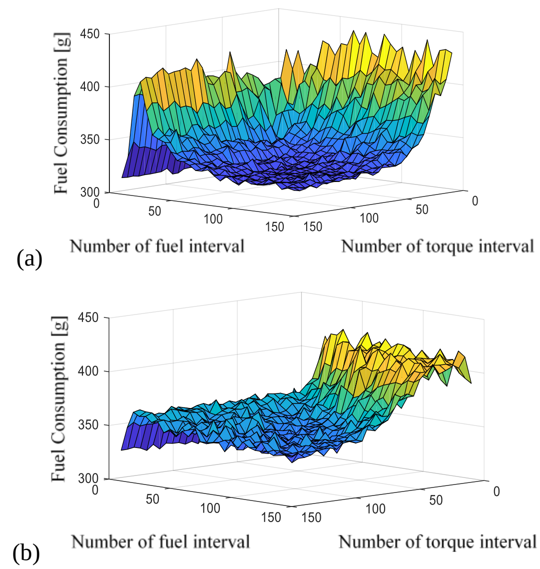

Fig. 6: Tuning parameters dependency of multimode implementation of SERCA for two different powertrain arrangements on UDDS driving cycle.

method is also capable of avoiding excessive mode changes beside being more consistent on tuning parameters.

VI. THE SERCA$^+$ ALGORITHM

In the previous sections, two applicable algorithms for EMS design of multimode power-split HEV powertrains have been reviewed. Both are characterized by weaknesses and strengths. In fact, PEARS is consistent but does not always show closeness with the global optimum, while SERCA is fast but strongly depends on tuning parameters, and mode trajectory can have unreasonably frequent mode changes. Consequently, the idea is to combine the two approaches to generate a strategy which outperforms both. Particularly, we use the stability of PEARS to determine the mode selection, in combination with the stepwise procedure of SERCA to determine the power split and near-optimal working conditions. The logic of the new method obtained, called SERCA$^+$, is reported as follows.

1) STEP 1: Data Preparation

At each driving cycle point, the best EV mode is selected with its relative working condition. For the HEV mode, the SERCA envelope is built and filtered. Once the profile is

convex, unlike SERCA, the PEARS based efficiency (11) is computed for each point. All the achievable HEV modes are then labelled by the highest achievable PEARS efficiency only.

2) STEP 2: PEARS mode selection

In this step, we obtain the mode trajectory for the driving cycle. First, at each driving cycle point, the HEV mode with the highest labelled efficiency is chosen. Next, rather than going ahead and finalizing the chosen mode, to prevent excessive mode changes (12)[29], we prefer the mode selected at the previous time step if its efficiency is comparable with the current highest identified efficiency.

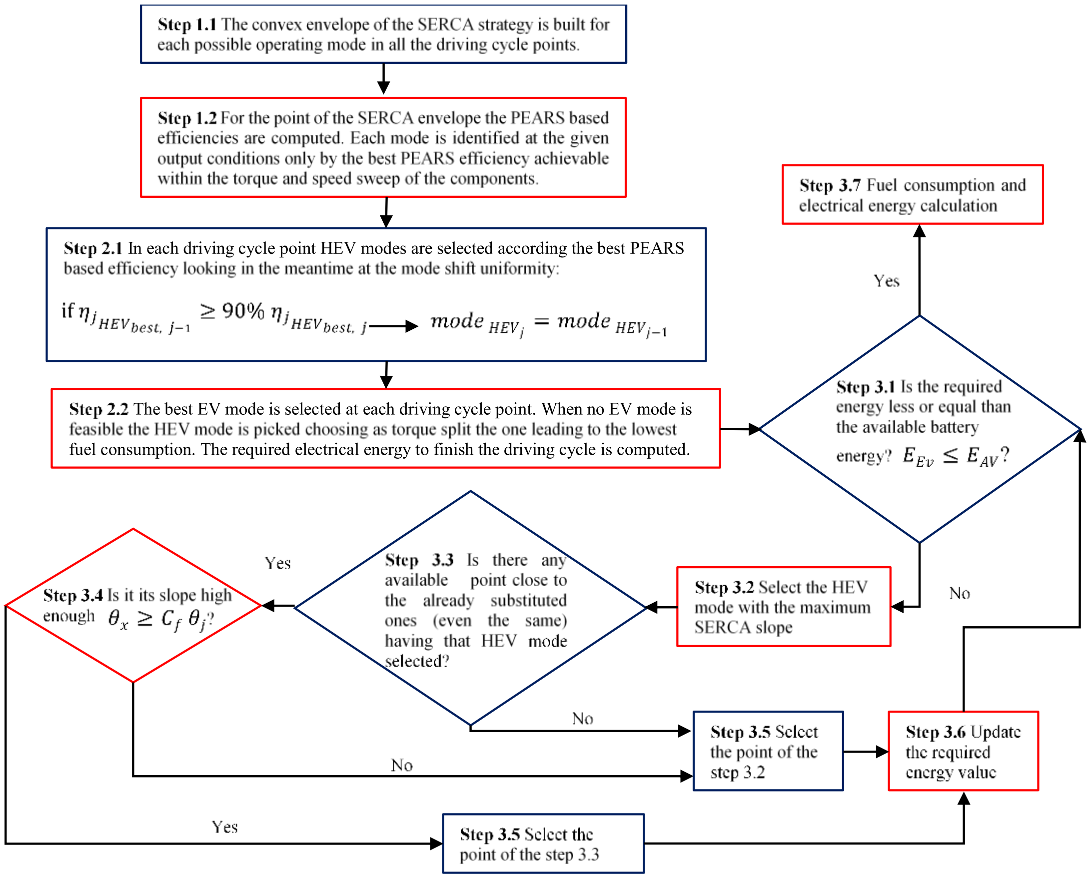

Fig.7. SERCA+ algorithm flowchart.

$$\text{if} \quad \eta_{HEV,best}[\mathrm{k}-1] \geq 90\%\ \eta_{HEV,best}[\mathrm{k}] \qquad (12)$$

$$\text{then} \quad mode_{\ HEV}[\mathrm{k}] = mode_{\ HEV}[k-1]$$

Note that this step totally differs with SERCA procedure, and unlike SERCA, PEARS-based mode identifying occurs in this stage of SERCA+. This step substantially improves final mode trajectories.

3) *STEP 3: Energy Balance Realization*

At first, the required electrical energy to complete the whole driving cycle in pure electric conditions is computed. Unlike the "multimode" SERCA illustrated in the previous section, since the operative modes have already been chosen in the previous step, only a single convex envelope exists at each driving cycle point. The HEV modes are then iteratively selected for the substitution based on the steepest SERCA slope.

The SERCA+ procedure explained in this section is schematically reported in the flowchart of Fig. 7. To show the benefits of the new methodology in terms of consistency and the robustness, we investigate the sensitivity to the tuning parameters. The fuel consumption fluctuations for the same architectures presented in the SERCA section are shown again in Fig.8 for SERCA+ for two different powertrain arrangements. SERCA+ shows considerably less dependence on the tuning parameters for both cases. We also observe a similar trend for other investigated arrangements.

VII. Case Study: State-of-the-Art Architecture

In this section, we compare the performance of different control algorithms on a state-of-the-art powertrain [32]. It should be noted that we only refer to the powertrain arrangement (Fig. 9), while using reasonable imaginary vehicle parameters and powertrain components As it is shown in Fig. 9, there exist three clutches in this arrangement, which potentially can generate eight different modes of operation. However, only five modes are practical. Clutch states for each of these five modes are shown in Table II.

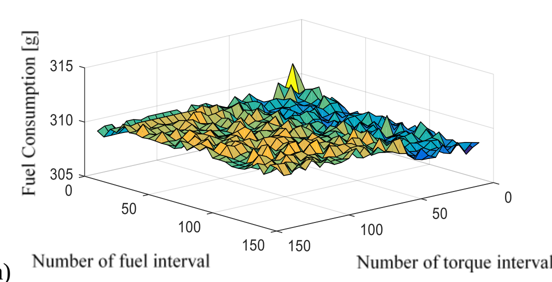

(a)

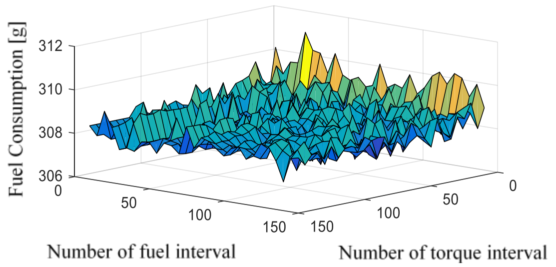

(b)

Fig.8: Tuning parameter dependency of SERCA+ for two different powertrain arrangements on UDDS driving cycle.

TABLE II
MODES OF OPERATION

Mode #	Description	Clutch State		
		CL1	CL2	CL3
1	Pure electric #1	1	1	0
2	Pure electric #2	1	0	1
3	Input split	0	0	1
4	Compound split	0	1	0
5	Parallel with fixed-gear ratio	0	1	1

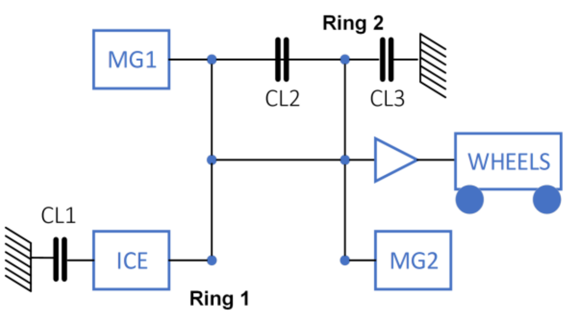

Fig. 9: State-of-the-art powertrain architecture

The objective of this section is to compare the different control strategies on the same powertrain arrangement to highlight the benefits of SERCA⁺. The evaluation is carried out on the HWFET and UDDS driving cycles.

Compared energy management strategies are SERCA+ which is introduced in this article, SERCA [21], modified PEARS presented in [29], and Dynamic Programming [33]. Results for each case are obtained using a desktop computer with Intel® Core™ i7-6700 (3.40GHz) and 32 GB of RAM.

The comparison shown in Table III highlights the benefit of the SERCA⁺ algorithm compared to the other strategies.in terms of predicted fuel consumption, computational time, and the total number of mode shifts. The augmented fuel consumption, SOC, and mode trajectories for two different driving cycles are also illustrated in Fig. 10. As shown in this table, although SERCA+ is slightly slower than PEARS and SERCA to elaborate the EMS, corresponding results demonstrate enhanced fuel economy. Results of SERCA+ are in fact 3.4% and 7.1% more efficient than SERCA and PEARS results for the highway driving cycle, respectively, and 1.1% and 10.2% more efficient for UDDS. Sub-optimality of

TABLE III
STRATEGIES COMPARISON

Strategy	Fuel Consumption [g]		CPU Time [s]		# of Mode Shifts	
	HWFET	UDDS	HWFET	UDDS	HWFET	UDDS
DP	593.9	309.9	2520	4380	179	417
PEARS	642.3	347.6	39	73	14	35
SERCA	617.4	315.6	114	108	235	536
SERCA+	596.4	312.2	140	145	22	42

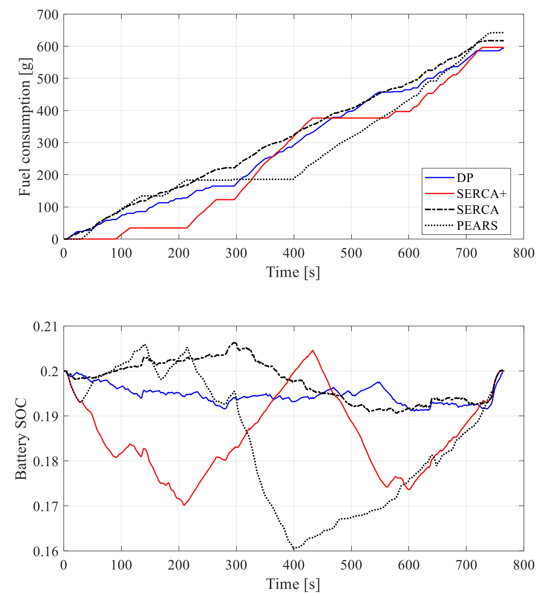

(a)

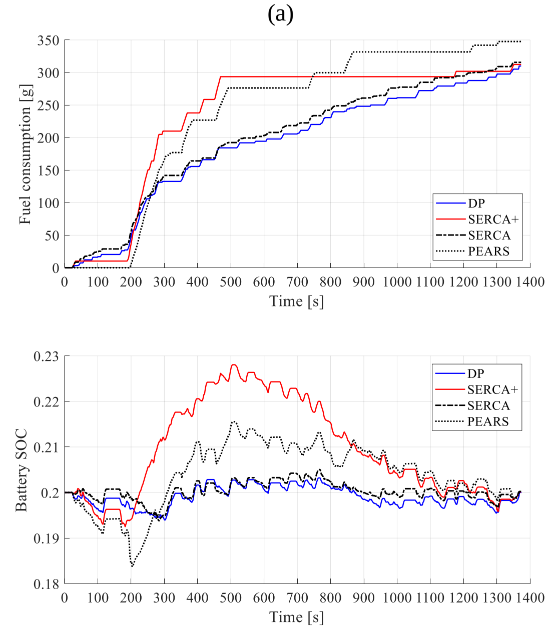

(b)

Fig. 10: Augmented fuel consumption and SOC trajectories of various algorithms for (a) HWFET and (b) UDDS driving cycles.

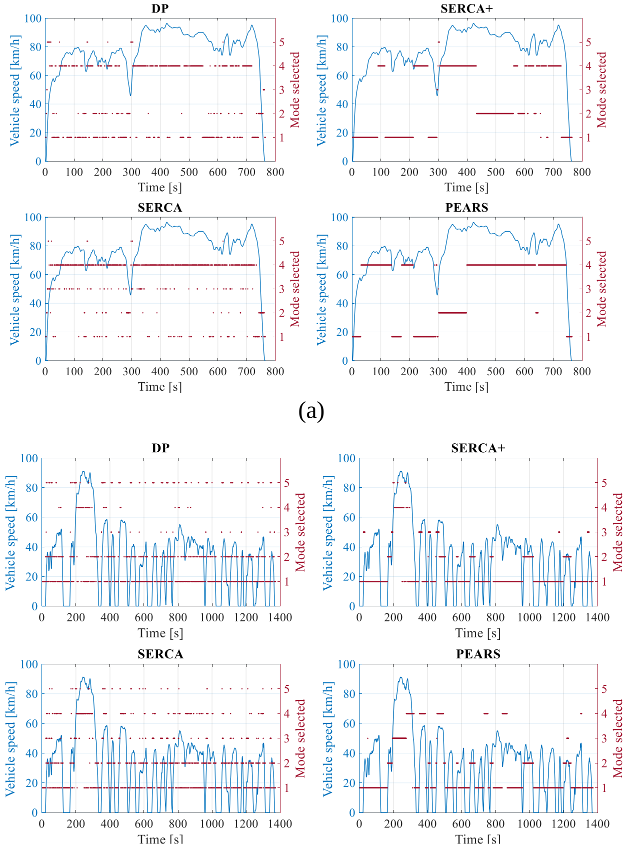

(a)

(b)

Fig. 11: Selected powertrain modes of different algorithms for (a) HWFET and (b) UDDS driving cycles

SERCA+ results is also demonstrated by generating at most 0.4% and 0.7% less fuel-efficient results compared to DP. In terms of the total number of mode shifts, it is evident that SERCA+ outperforms both SERCA and DP by a large margin. This is illustrated in Fig. 11, where powertrain mode trajectories are shown for two driving cycles. This advantage of SERCA+ is mostly due to using (12). Fig. 12 shows the presented results in Table III graphically. This figure is helpful to observe that SERCA+ is placed in a middle position between strategies as DP, characterized by good performances but higher computational cost, and as PEARS, converging extremely quickly to a solution, but with discrepancy with the benchmark.

This also shows that SERCA+ benefits from three main advantages, which are optimality of DP, swiftness of SERCA, and mode management of PEARS. In the previous section, we have also observed that SERCA+ is less dependent on the tuning parameters. All mentioned characteristics make the

SERCA+ algorithm an outstanding trade-off between robustness, sub-optimality, computation time, and the feasibility (excessive mode change avoidance). To conclude, we obtained this trend for a six modes application which confirms the value of the proposed solution. We propose that SERCA+ addresses the problem of the multimode power-split HEV powertrains design.

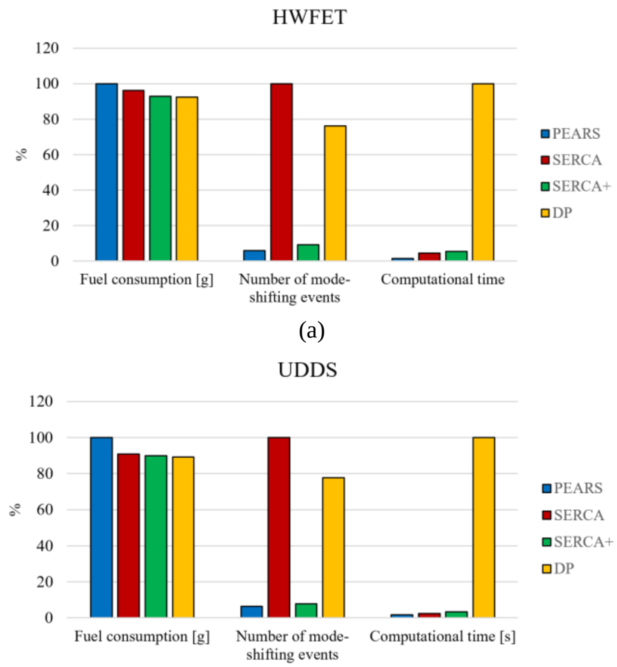

(a)

(b)

Fig. 12: Comparison of SERCA+, SERCA, PEARS, and DP on (a) HWFET and (b) UDDS driving cycles.

VIII. CONCLUSION

In this paper, we have presented a new approach to deal with the energy management problem for a multimode power-split HEV. The proposed algorithm, called SERCA$^+$, is consistent and quickly produces good quality results compared to the globally optimal solution. This algorithm elaborates more data to select the working conditions, yet this does not compromise the computational cost, which has been proven to increase only by a marginal extent compared to the PEARS strategy. Furthermore, the comparison with the other methods has highlighted the clear advantage of the proposed approach in terms of predicted fuel consumption and reasonable mode changes. All these evidences make the SERCA$^+$ a perfect candidate as a new strategy to be applied in the design problem of multimode power split HEVs, where a rapid and precise evaluation of a large pool of candidates is required.

REFERENCES

[1] A. Emadi, “Transportation 2.0: Electrified-Enabling cleaner, greener, and more affordable domestic electricity to replace petroleum,” in *IEEE Power Energy Mag.*, vol. 9, no. 4, pp. 18–29, 2011.

[2] B. Bilgin, P. Magne, P. Malysz, Y. Yang, V. Pantelic, M. Preindl, A. Korobkine, W. Jiang, M. Lawford, and A. Emadi, “Making the Case for Electrified Transportation,” *IEEE Transactions on Transportation Electrification*, vol. 1, no. 1, pp. 4–17, 2015.

[3] A. Emadi, K. Rajashekara, S. S. Williamson e S. Lukic, “Topological Overview of Hybrid Electric and Fuel Cell Vehicular Power System Architectures and Configurations,” *Vehicular Technology, IEEE Transactions*, vol. 54, pp. 763-770, 2005.

[4] C. Chan, “The State of the Art of Electric, Hybrid, and Fuel Cell Vehicles,” *Proceedings of the IEEE*, vol. 95, pp. 704-718, 2007.

[5] B. Mashadi and S. A. M. Emadi, "Dual-Mode Power-Split Transmission for Hybrid Electric Vehicles," in *IEEE Transactions on Vehicular Technology*, vol. 59, no. 7, pp. 3223-3232, 2010.
[6] I. J. Albert, E. Kahrimanovic, and A. Emadi, "Diesel Sport Utility Vehicles With Hybrid Electric Drive Trains," in *IEEE Transactions on Vehicular Technology*, vol. 53, No. 4 pp. 1247–1256, 2004.
[7] A. I. Antoniou, J. Komyathy, J. Bench and A. Emadi, "Modeling and Simulation of Various Hybrid-Electric Configurations of the High-Mobility Multipurpose Wheeled Vehicle (HMMWV)," in *IEEE Transactions on Vehicular Technology*, vol. 56, no. 2, pp. 459-465, March 2007.
[8] S. S. Williamson, S. G. Wirasingha, and A. Emadi, "Comparative Investigation of Series and Parallel Hybrid Electric Drive Trains for Heavy-Duty Transit Bus Applications," in *Conf. IEEE-VPPC*, pp. l-l0,2006
[9] Y. Yang, K. A. Ali, J. Roeleveld, and A. Emadi, "State-of-the-art electrified powertrains - hybrid, plug-in, and electric vehicles," *International Journal of Powertrains*, vol. 5, no. 1, p. 1, 2016.
[10] J. M. Miller, "Hybrid electric vehicle propulsion system architectures of the e-CVT type," *IEEE Transactions on Power Electronics*, vol. 21, n. 3, pp. 756-767, 2006
[11] S. Delprat, J. Lauber, T. M. Guerra, and J. Rimaux, "Control of a Parallel Hybrid Powertrain: Optimal Control," in *IEEE Transactions on Vehicular Technology*, vol. 53, no. 3, May 2004.
[12] Q. Gong, Y. Li and Z. R. Peng, "Trip-Based Optimal Power Management of Plug-in Hybrid Electric Vehicles," *IEEE Transactions on Vehicular Technology*, vol. 57, no. 6, pp. 3393-3401, Nov. 2008.
[13] J. Liu and H. Peng, "Modelling and Control of a Power-Split Hybrid Vehicle, "*IEEE Transactions on Control Systems Technology*, vol. 16, no. 6, pp. 1242-1251, 2008.
[14] X. Zhang, S. Eben Li, H. Peng e J. Sun, "Efficient Exhaustive Search of Power-Split Hybrid Powertrains With Multiple Planetary Gears and Clutches," *Journal of Dynamic Systems Measurement and Control*, vol. 137, n. 12, 2015.
[15] R. E. Bellman, *Dynamic programming*. Princeton - N.J.: Princeton University Press, 1957.
[16] G. Paganelli, G. Ercole, A. Brahma, Y. Guezennec, G. Rizzoni, "General supervisory control policy for the energy optimization of charge-sustaining hybrid electric vehicles," *JSAE Review*, vol. 22, no. 4, pp. 511–518, 2001.
[17] N. Kim, S. Cha, and H. Peng, "Optimal Control of Hybrid Electric Vehicles Based on Pontryagin's Minimum Principle," *IEEE Transactions on Control Systems Technology*, vol. 19, no. 5, pp. 1279-1287, Sept. 2011.
[18] L. Serrao, S. Onori, and G. Rizzoni. "A comparative analysis of energy management strategies for hybrid electric vehicles," *Journal of Dynamic Systems, Measurement, and Control*, vol. 133, 2011
[19] X. Zhang, H. Peng, and J. Sun, "A near-optimal power management strategy for rapid component sizing of power split hybrid vehicles with multiple operating modes," *American Control Conference (ACC)*, pp. 5972-5977, 2013.
[20] X. Zhang, S. E. Li, H. Peng and J. Sun, "Design of Multimode Power-Split Hybrid Vehicles—A Case Study on the Voltec Powertrain System," IEEE *Transactions on Vehicular Technology*, vol. 65, no. 6, pp. 4790-4801, June 2016.
[21] P. G. Anselma, Y. Huo, J. Roeleveld, G. Belingardi and A. Emadi, "Slope-Weighted Energy-Based Rapid Control Analysis for Hybrid Electric Vehicles," in IEEE Transactions on Vehicular Technology, vol. 68, no. 5, pp. 4458-4466, May 2019.
[22] H. Benford and M. Leising, "The Lever Analogy: A New Tool in Transmission Analysis," *SAE Technical Paper*, 1981
[23] L. Jinming and H. Peng, "A systematic design approach for two planetary gear split hybrid vehicles," *Vehicle System Dynamics*, 48:11, pp. 1395-1412, 2010
[24] Y. Yang and A. Emadi, "Integrated electro-mechanical transmission systems in hybrid electric vehicles," IEEE *Vehicle Power and Propulsion Conference*, Chicago, IL, pp. 1-6,2011
[25] W. Zhuang, X. Zhang, Y. Ding, L. Wang, and X. Hu, "Comparison of multi-mode hybrid powertrains with multiple planetary gears," *Applied Energy*, vol. 178, pp. 624-632, 2016.
[26] W. Zhuang, X. Zhang, D. Li, L. Wang, G. Yin, "Mode shift map design and integrated energy management control of a multi-mode hybrid electric vehicle," *Applied Energy*, vol. 204, pp. 476-488, 2017
[27] X. Zhang, S. E. Li, H. Peng, J. Sun, "Efficient Exhaustive Search of Power-Split Hybrid Powertrains with Multiple Planetary Gears and Clutches," *Journal of Dynamic Systems, Measurement, and Control*, vol. 137, no. 12, 2015.
[28] X. Zhang, S. E. Li, H. Peng, and J. Sun, "Design of Multimode Power-Split Hybrid Vehicles—A Case Study on the Voltec Powertrain System," IEEE *Transactions on Vehicular Technology*, vol. 65, no. 6, pp. 4790-4801, June 2016.
[29] P. G. Anselma, Y. Huo, A. Edris, J. Roeleveld, A. Emadi, and G. Belingardi. "Mode-shifting Minimization in a Power Management Strategy for Rapid Component Sizing of Multimode Power Split Hybrid Vehicles," *SAE Technical Paper 2018-01-1018*, Mar. 2018.
[30] P.G. Anselma, Y. Huo, J. Roeleveld, A. Emadi, and G. Belingardi. "Rapid optimal design of a multimode power split hybrid electric vehicle transmission," *Proceedings of the Institution of Mechanical Engineers Part D Journal of Automobile Engineering*, vol. 233, no. 3, pp. 740-762, 2019.
[31] K. Ahn, S. Cho, and S. W. Cha, "Optimal operation of the power-split hybrid electric vehicle powertrain," *Proceedings of the Institution of Mechanical Engineers, Part D: Journal of Automobile Engineering*, vol. 222, no. 5, pp. 789-800, 2008.
[32] M.A. Miller, A.G. Holmes, B.M. Conlon, and P.J Savagian, "The GM "Voltec" 4ET50 Multi-Mode Electric Transaxle," *SAE International Journal of Engines*, vol.4, pp. 1102-1114, 2011
[33] O. Sundstrom and L. Guzzella, "A generic dynamic programming Matlab function," *2009 IEEE Control Applications, (CCA) & Intelligent Control, (ISIC)*, pp. 1625-1630, 2009.

Giuseppe Buccoliero received the B.S. and M.S. in mechanical engineering with merits from Politecnico di Torino, Italy, in 2016 and 2018 respectively.
In 2018 he has been a master's student researcher at the McMaster Institute for Automotive Research and Technology in Hamilton, ON, Canada. He is currently pursuing a Master of Business Administration (MBA) at Collège des Ingénieurs (Paris, Munich, Turin).

Pier Giuseppe Anselma (S'18) received the B.S. and M.S. in mechanical engineering with merits from Politecnico di Torino, Italy, in 2014 and 2017 respectively. He is currently working towards the Ph.D. degree in mechanical engineering at Politecnico di Torino.
In 2016 and in 2019 he has been respectively a master's student researcher and a visiting Ph. D. student researcher at the McMaster Institute for Automotive Research and Technology in Hamilton, ON, Canada, where he developed his interest towards the electrification of road vehicles.
At present, he his author and co-author of around 15 peer-reviewed conference and journal publications. His research activities involve design of powertrains and implementation of smart energy management strategies related to electrified and connected vehicles.

Saeed Amirfarhangi Bonab received the B.S. in Mechanical Engineering in 2017 from Sharif University of Technology, Tehran, Iran, and the M.S. in Mechanical Engineering from McMaster University, Hamilton, ON, Canada, in 2019. He had been working on the vehicular technologies for the next generation transportation with McMaster Automotive Resource Centre, from 2017 to 2019. His main topic of interest is the application of optimization and control of dynamic systems in autonomous driving and powertrain electrification.

Giovanni Belingardi received the M.S. degree in Mechanical Engineering from Politecnico di Torino in 1975.
From 1977 to 1983 he joined the Technical Department of FIAT Auto. Then he came back to Politecnico di Torino and joined the Mechanical Engineering Department as Assistant Professor. Here he developed his academic carrier up to his present position of full Professor.
He is author of more than 280 papers published in international scientific journals and in proceedings of national and international conferences.
He has recently been and at present is the scientific coordinator of the Operative Units of the Mechanical and Aerospace Engineering Department for a number of projects of the framework programs of the European Union, of the National and Regional Governments. Research cooperation with industrial partners has been effective as well.
He is the responsible for International cooperation of Politecnico di Torino within the frame of the Automotive Engineering, with particular attention toward Canada, US, Brazil, Poland and Serbia. Quite frequent visits of those countries give him a special insight of their situation and needs and allowed him to construct a wide net of partnership.

Ali Emadi (IEEE S'98-M'00-SM'03-F'13) received the B.S. and M.S. degrees in electrical engineering with highest distinction from Sharif University of Technology, Tehran, Iran, in 1995 and 1997, respectively, and the Ph.D. degree in electrical engineering from Texas A&M University, College Station, TX, USA, in 2000. He is the Canada Excellence Research Chair Laureate at McMaster University in Hamilton, Ontario, Canada. He is also the holder of the NSERC/FCA Industrial Research Chair in Electrified Powertrains and Tier I Canada Research Chair in Transportation Electrification and Smart Mobility. Before joining McMaster University, Dr. Emadi was the Harris Perlstein Endowed Chair Professor of Engineering and Director of the Electric Power and Power Electronics Center and Grainger Laboratories at Illinois Institute of Technology in Chicago, where he established research and teaching facilities as well as courses in power electronics, motor drives, and vehicular power systems. He was the Founder, Chairman, and President of Hybrid Electric Vehicle Technologies, Inc. (HEVT) – a university spin-off company of Illinois Tech. Dr. Emadi has been the recipient of numerous awards and recognitions. He was the advisor for the Formula Hybrid Teams at Illinois Tech and McMaster University, which won the GM Best Engineered Hybrid System Award at the 2010, 2013, and 2015 competitions. He is the principal author/coauthor of over 450 journal and conference papers as well as several books including *Vehicular Electric Power Systems* (2003), *Energy Efficient Electric Motors* (2004), *Uninterruptible Power Supplies and Active Filters* (2004), *Modern Electric, Hybrid Electric, and Fuel Cell Vehicles* (2nd ed, 2009), and *Integrated Power Electronic Converters and Digital Control* (2009). He is also the editor of the *Handbook of Automotive Power Electronics and Motor Drives* (2005) and *Advanced Electric Drive Vehicles* (2014). He is the co-editor of the *Switched Reluctance Motor Drives* (2018). Dr. Emadi was the Inaugural General Chair of the 2012 IEEE Transportation Electrification Conference and Expo (ITEC) and has chaired several IEEE and SAE conferences in the areas of vehicle power and propulsion. He is the founding Editor-in-Chief of the *IEEE Transactions on Transportation Electrification*.